Mathematics and Mechanics of Granular Materials

Edited by

JAMES M. HILL

University of Wollongong, Australia

and

A.P.S. SELVADURAI

McGill Univeristy, Montreal, ON, Canada

Reprinted from *Journal of Engineering Mathematics,* Vol. 52, Nos. 1–3 (July 2005)

Springer

Library of Congress Cataloging-in-Publication Data

ISBN 1-4020-3781-3

Published by Springer,
P.O. Box 17, 3300 AA Dordrecht, The Netherlands.

Printed on acid-free paper

Printed in the Netherlands

TABLE OF CONTENTS

Journal of Engineering Mathematics (2005) 52: 1–9
DOI 10.1007/s10665-005-2729-1

Mathematics and mechanics of granular materials

J.M. HILL and A.P.S. SELVADURAI[1]
School of Mathematics and Applied Statistics, University of Wollongong, Wollongong, NSW, Australia (jhill@uow.edu.au); [1]*McGill University, Montreal, QC, Canada (patrick.selvadurai@mcgill.ca)*

Received and accepted 10 February 2005

The study of granular materials has always been a topic of considerable importance in engineering. Historically, the mathematical formulation of the subject dates back to the pioneering work of C.A. Coulomb in 1776 [1]. In his now famous memoir, Coulomb postulated the conditions that should be satisfied for failure to occur in a granular material. This postulate for failure still stands as a defining point in the mathematical study of mechanics of granular materials. Coulomb largely focused on a topic of importance to that time, namely the design of earth structures to avoid collapse. As a result, the study of the deformations that lead to failure received less emphasis [2]. Recently, however, several scientific disciplines, including geomechanics, mechanical, civil and chemical engineering, physics and applied mathematics, have shown renewed interest in accurately modelling granular materials to examine, concurrently, both failure and deformations. The study of how granular materials or bulk solids flow and deform is also of practical importance for a number of industries, including mining and minerals processing, agricultural materials processing, the construction industry, foodstuff production, pharmaceutical development and nanotechnology. In these applications the granular materials involved could be as diverse as crushed ore, cereal grains, sugar, flour, tablets and nano-particulates. In each case, granular materials frequently flow through devices such as bins, hoppers and chutes and a clear knowledge of how they behave under these circumstances is invaluable for the efficient design and application of related devices.

Granular materials form an important component in modern developments in geomechanics. For the most part, geotechnical engineers are less interested in fully developed granular flows, but the deformational aspects of granular materials are highly relevant in situations that require assessment of settlements of foundations on granular media. The development of mathematically correct and physically admissible theories to describe and predict the complex behaviour of granular materials or bulk solids is therefore a topic of fundamental importance to both the engineering sciences and applied mathematics.

Modelling the flow of granular materials has been extensively studied through the use of continuum mechanics. Using this approach, one formulates governing equations for the stress and velocity fields by coupling the equations of conservation of mass and linear momentum with appropriate constitutive laws that govern the initiation of failure and the rules applicable to the flow of the granular material subsequent to its failure. For rapid granular flows that accompany a reduction in the bulk density, the behaviour of each granular particle is determined primarily by inelastic collisions with neighbouring particles, in a way analogous to colliding molecules in dense gases. In contrast, for slow dense granular flows, the dominant

mechanisms are quite different; here, the neighbouring particles continually slide and roll past each other, and friction between these particles becomes the dominant force.

The problem of modelling fully developed slow granular flows using continuum mechanics is, and continues to be, both complex and challenging. There is general agreement that stress fields within granular flows can be described by coupling the equations of linear momentum with the Coulomb–Mohr yield condition, or other forms of yield condition applicable to the myriad of granular materials that are encountered in engineering practice. However, there is little or no agreement as to how the equations for the velocity fields, that describe the deformations of fully developed flows, should be formulated, or even whether these equations should be mathematically well-posed or ill-posed. The constitutive assumption that is perhaps most widely employed by the engineering community is Saint-Venant's hypothesis, which is also referred to as the coaxiality condition. This condition states that the principal axes of the stress and strain-rate tensors should coincide. Drucker and Prager [3] were the first to formally adopt this hypothesis for the study of the mechanics of granular materials. They used the Coulomb–Mohr yield condition as a plastic potential to derive an associated flow rule. The condition of coaxiality must hold by virtue of material isotropy, and the rate-of-strain tensor depends only on the Cauchy stress tensor.

While the work of Drucker and Prager [3] marks the resurgence of the application of plasticity theories to mechanics of soils, these developments have limitations. Firstly, the theory predicts that all granular flows are accompanied by dilation or volume change, notably volume expansion, whereas in fact loose granular materials contract upon shearing, and others undergo isochoric or volume-preserving deformations. Even in situations for which dilation is appropriate, the predicted magnitude of volume increases is far in excess of those observed in most real materials. The second limitation is that for cohesionless materials; the theory predicts that the rate of specific mechanical energy dissipation is zero, which is clearly unrealistic. More sophisticated approaches attempt to overcome these difficulties by either including work-hardening/softening theories, similar to those proposed and developed by Drucker *et al.* [4], Jenike and Shield [5], Schofield and Wroth [6] or the incorporation of flow rules that are non-associated. In the former category of models, the yield condition varies with a state parameter, such as the density. For the work-hardening/softening models, the mathematical characteristics for the stress and velocity fields do not coincide, contrary to what is commonly observed experimentally; this leads to the adoption of non-associated flow rules. The subject matter in this area is extensive and no attempt will be made to provide an exhaustive review of non-associated plasticity. It is worth noting that Hill [7] proposed velocity equations for incompressible materials based on the Saint-Venant hypothesis, but, again, this theory has the undesirable property that the predicted stress and velocity characteristics do not coincide.

By abandoning the assumption of coaxiality, an alternative family of models has been derived based on a kinematic hypothesis involving the concepts of shearing motion parallel to a surface, rotation of that surface, and dilation or contraction normal to the surface. One such model is the double-shearing theory, originally proposed by Spencer [8, 9] for incompressible flows, and extended to dilatant materials by Mehrabadi and Cowin [10] and Butterfield and Harkness [11]. In this theory, the characteristic curves for the stresses and velocities coincide, and every deformation is assumed to consist of simultaneous shears along the two families of stress characteristics. These ideas build upon those of the double sliding, free rotating model, developed by de Josselin de Jong [12–14], by fixing the rotation rate as the temporal rate of change of the stress angle. To reiterate, an important advantage of the double-shearing theory over the previous coaxial theories is that it retains the assumption of

slip occurring along the stress characteristics, but does not give rise to unusually high levels of dilatancy. Spencer's [8, 9] original double-shearing theory is for incompressible materials, which in the context of fully developed granular flow is often a reasonable and a realistic assumption. Furthermore, when applied to gravity-driven flow problems [15, 16], the coaxial theory is shown to yield physically unacceptable predictions in the velocity field, whereas the double-shearing theory predicts results that are certainly reasonable. On the other hand, there are experiments, which are not consistent with predictions of Spencer's double-shearing theory, but tend to support the double-sliding, free-rotating model of de Josselin de Jong [12–14]. Research in this area must recognize the fact that there is little possibility for developing a mathematical theory of granular media for all eventualities: the materials are real and the circumstances diverse. A theory that shows promise for a given set of experimental conditions can fail for others. In any event, at this moment no single theory is clearly most applicable for describing the behaviour of fully developed flow of real granular materials. While the subject requires more reproducible non-conventional experiments to help resolve these issues, there is a serious need for in-depth mathematical and numerical analysis of the theories involved. This might include the solution of relevant boundary-value problems and initial-boundary-value problems that can allow the continuous transformation of a deformation-dominated process to a flow-dominated one, the exploration of exact and numerical solutions to the equations, and the comparison and contrasting of existing theories that will guide critical experiments of the future.

In addition to the issues raised above, a major unresolved question with Spencer's [8, 9] double-shearing theory, and most other plasticity-based theories for fully developed granular flow, is that the equations are linearly ill-posed in the sense that small perturbations to existing solutions may result in solutions that grow exponentially with time (see *e.g.* [17–19]). This characteristic places doubt on whether or not steady solutions to the governing equations actually describe real granular flows, and also leads to serious implications for numerical schemes, which do not converge in the limit as the size of a mesh discretization approaches zero. However, ill-posedness in itself is not necessarily an undesirable property for equations that describe granular deformations. In fact, it is well known that under certain circumstances granular materials exhibit unstable behaviour, in which case it is quite plausible that ill-posedness should be the norm. An example is the onset of shear-banding. Perhaps the ideal situation, as advocated by Harris [19], is a theory that contains a domain of well-posedness, in which solutions may be stable or unstable, and also a domain of ill-posedness, which corresponds to a definite physical instability. This motivation has led Harris [20, 21] to derive a single-slip model, which belongs to the class of models based upon the physical and kinematic considerations discussed above. This single-slip model is indeed well-posed under well-defined conditions and ill-posed when these conditions fail [19]. In this case the ill-posedness corresponds to the physical instability of grain separation, a process that invalidates the assumption that friction between particles is the dominant mode of momentum transfer, as opposed to inelastic collisions. There is much scope for further research in this complex and challenging field.

We note that there have been several recent attempts to model the transitional region between dense, slow granular flows and rapid, collisional flows (see, for example, [22–25]. These models combine traditional plasticity ideas with notions borrowed from the kinetic theory of gases [26]. In general, the condition of coaxiality is enforced, and again it is not entirely clear whether these theories are well-posed or ill-posed. Often in fully developed slow granular flow, there are narrow layers, referred to as shear layers, in which the material experiences intense shearing. While the models mentioned previously capture many features of fully

developed flow to varying degrees, none have the ability to accurately predict the thickness of the layers over which such intense shearing materializes. A reason for this limitation has been attributed to the fact that classical continuum models have no intrinsic length scale built into the constitutive equations. Attempts to rectify this deficiency probably date back to the work of Voigt [27] and later expanded by Cosserat and Cosserat [28] who introduced the concept of couple stresses for examining the mechanics of deformable media (see *e.g.* [29]). Here, the Cauchy stress tensor is no longer symmetric, and the conservation of angular momentum is no longer automatically satisfied but becomes a set of field equations that need to be satisfied explicitly. There are two extra field variables for Cosserat materials, namely the angular velocity and the couple-stress tensor. As a consequence of the notion of couple stresses, a length parameter or an intrinsic length scale naturally arises in the definition of constitutive relationships. The work on both micromorphic and couple-stress theories was an active area of research from the mid-1960s to the mid-1970s and the developments are summarized in [30]. A number of authors have applied these concepts to the examination of problems associated with granular media and references to recent works are given by Vardoulakis and Sulem [31]. The investigations by Mühlhaus [32], Tejchman and Wu [33], Bauer [34], Tejchman and Bauer [35], Tejchman and Gudehus [36] and others also deal with the application of higher-order formulations in elastoplasticity, in the context of the theory of hypoplasticity, which is described below, and by Mohan *et al*. [37, 38] who use more traditional ideas from plasticity. In each case, this improvement is achieved by modelling the granular material as a Cosserat (or micropolar) continuum. Mohan *et al*. [37, 38] apply an extended-associated flow rule, with the yield condition depending on the bulk density, and apply the equations to model flow through vertical channels and cylindrical Couette flow. These studies are successful in that they predict the main qualitative features of the shear layers; however, the yield condition and flow rule were chosen purely for illustrating the effectiveness of this approach.

In many civil and geotechnical engineering applications the constrained response of a granular material, such as a soil or sand, under loading is most important [29]. Examples of such situations occur with the analysis of foundations, excavations and underground structures, or simply in elemental tests. Here, the deformation of the material is contained by a surrounding material, which prevents the development of a state of plastic flow or collapse. Traditionally, a variety of elastoplastic models have been applied to problems of this nature. The history of development of theories of geomaterial behaviour that account for contained deformations of granular materials is quite extensive, and no attempt will be made here to provide an all-encompassing review. More recently, however, the constitutive theory of hypoplasticity has been developed, and has proven to be an attractive alternative to the elastoplastic models. Hypoplasticity is a natural extension of the theories of hypoelasticity developed by Truesdell [40] and the connection between the theories of hypoelasticity and theories of plasticity and of elastic-plastic flow has been discussed and investigated by Green [41, 42], Truesdell and Noll [43] and Jaunzemis [44]. Hypoplasticity in a formal sense was extensively investigated by Kolymbas [45] and many co-workers (see [46–48]). The characterizing feature of all hypoplastic theories is that the constitutive law can be written in a single nonlinear tensorial equation for the stress-rate as a function of the stress and the rate-of-deformation tensor, without reference to a yield condition or a flow rule. With hypoplasticity there is no need to decompose deformations into elastic and plastic regimes *a priori*, or to distinguish between loading and unloading; all these notions are automatically built into the theory, and arise as a consequence. Excellent reviews of hypoplasticity and its development are contained in Kolymbas [49] and Wu and Kolymbas [50].

The popularity of hypoplasticity among researchers and practitioners can be attributed to its elegance and the fact that the theory is deeply rooted in experimental observations. It is, nonetheless, a sophisticated constitutive theory, which involves complicated nonlinear constitutive relationships. When combined with the governing equations of continuum mechanics, there are little prospects for the analytical solution of real-life boundary-value problems, and progress is usually made via numerical schemes. As a result, it is often difficult to grasp the underlying mathematical structure of the equations (see [51–54]).

As mentioned previously, for each particular hypoplastic law there is a yield surface and a flow rule, but rather than being assigned in advance, they are consequences of the original constitutive relationships. Thus hypoplasticity as a theory can, in principle, be used to model fully developed granular flow. The explicit equations describing the yield condition and the flow rule can be derived from the given hypoplastic law, as illustrated by Wu and Niemunis [55] and von Wolffersdorff [56]. Von Wolffersdorff [56] has derived particular hypoplastic models that give the yield surfaces of Drucker and Prager [3] and Matsuoka and Nakai [57] as limiting cases. It is not immediately clear whether a similar derivation can be made to link hypoplasticity with other plasticity theories such as the double-shearing theory [8–10] described above. This possibility is of considerable interest, especially in light of the recent work of Spencer [58], who shows that in a strict sense, the double-shearing theory can be regarded as a special form of hypoplasticity. There is an absence of understanding of the strict connection between hypoplasticity and theories of plasticity that describe granular flow.

Shear layers often occur in the vicinity of solid boundaries, but this is not generally the case. An important property of granular materials is that shear-banding or shear layers can also occur within the bulk of the material. Shear bands are usually accompanied by localised strains, spanning several grain diameters in thickness, and as discussed above, classical continuum approaches fail to account for the dimensions of the shear bands due to the absence of an intrinsic length-scale. Furthermore, although the onset of shear-banding can be predicted [59], the ill-posedness of the governing equations prevents a complete analysis. As discussed previously, the subject of layers with intense shearing or shear-banding has received much attention by investigators who have developed approaches that incorporate Cosserat-type effects, and this is most prominent in hypoplasticity (see *e.g.* [34–36, 60]). Various hypoplastic theories have been developed and validated using finite-element techniques. The topic of mechanics and mathematics of granular materials has a rich history of involvement of researchers in the engineering sciences as well as those in the mechanics and applied-mathematics communities. These contributions are too numerous to cite as a comprehensive and complete review; readers are referred to the following Edited volumes of Symposia and Conference Proceedings for more in-depth reviews of the historical developments and the current state of advanced mathematical and mechanics approaches to the study of granular materials [61–78].

This Special Issue on the Mathematics and Mechanics of Granular Materials presents a mix of mathematical and engineering contributions to the discipline. Some of the papers, but not all, originate from four Mini-Symposia held at the 2003 ICIAM (International Congress of Industrial and Applied Mathematics) in Sydney, Australia, June 7–11, 2003. This meeting was jointly organised by the Guest Editors together with Drs. Claudio Tamagnini and Antoinette Tordesillas. The papers presented in this Special Issue cover the full range of current research activity in the area, and include general, analytical, hypoplastic, numerical and engineering contributions, but appear as follows according to the alphabetical listing of the first-named author:

1. F. Alonso-Marroquin and H.J. Herrmann, Investigation of the incremental response of soils using a discrete element model.
2. E. Bauer, Initial response of a micro-polar hypoplastic material under plane shearing.
3. R. Chambon, Some general results about second order work, uniqueness, existence and controllability.
4. G.M. Cox, S.W. McCue, N. Thamwattana and J. M. Hill, Perturbation solutions for flow through symmetrical hoppers with inserts and asymmetrical wedge hoppers.
5. B.S. Gardiner and A. Tordesillas, Micromechanical constitutive modelling of granular media: evolution and loss of contact in particle clusters.
6. D. Harris and E.F. Grekova, A hyperbolic well-posed model for the flow of granular materials.
7. S.C. Hendy, Towards a theory of granular plasticity.
8. M. Hjiaj, W. Huang, K. Krabbenhoft and S.W. Sloan, Formulation of non-standard dissipative behaviour of geomaterials.
9. W. Huang, M. Hjiaj and S.W. Sloan, Bifurcation analysis for shear localization in non-polar and micro-polar hypoplastic continua.
10. V.A. Osinov, Large-strain dynamic cavity expansion in a granular material.
11. E. Pasternak and H.-B. Muhlhaus, Generalised homogenisation procedures for granular materials.
12. J.F. Peters, Some fundamental aspects of the continuumization problem in granular media.
13. A.J.M. Spencer, Compression and shear of a layer of granular material.
14. C. Tamagnini, F. Calvetti and G. Viggiani, An assessment of plasticity theories for modelling the incrementally non–linear behavior of granular soils.
15. G.J. Weir, Incompressible granular flow from wedge-shaped hoppers.
16. H.P. Zhu and A.B. Yu, Micromechanics modeling and analysis of unsteady state granular flow in a cylindrical hopper.

Acknowledgements

The Guest Editors wish especially to acknowledge the help and assistance of a large number of people who acted as referees for this Special Issue, but particularly to Drs. Grant Cox and Scott McCue who cheerfully undertook many additional burdens.

References

1. C.A. Coulomb, Essai sur une application des règles *de maximis* & *minimis* à quelques problèmes de statique, relatifs à l'architecture, *Mémoire de Mathématique & de Physique, présentés à l'Académie Royale des Sciences par divers Savans, & lûs dans ses Assemblées*, Vol. 7, 1773, Paris (1776) pp. 343–382.
2. J. Heyman, *Coulomb's Memoir on Statics*. Cambridge: Cambridge University Press (1972) 212 pp.
3. D.C. Drucker and W. Prager, Soil mechanics and plastic analysis or limit design. *Q. Appl. Math*. 10 (1952) 157–165.
4. D.C. Drucker, R.E. Gibson and D.J. Henkel, Soil mechanics and work-hardening theories of plasticity. *Trans. ASCE* 122 (1957) 338–346.
5. A.W. Jenike and R.T. Shield, On the plastic flow of Coulomb solids beyond original failure. *J. Appl. Mech*. 26 (1959) 599–602.
6. A. Schofield and P. Wroth, *Critical State Soil Mechanics*. London: McGraw-Hill (1968) 310 pp.
7. R. Hill, *The Mathematical Theory of Plasticity*. Oxford: Clarendon Press (1950) 355 pp.
8. A.J.M. Spencer, A theory of the kinematics of ideal soils under plane strain conditions. *J. Mech. Phys. Solids* 12 (1964) 337–351.

9. A.J.M. Spencer, Deformation of ideal granular materials. In: H.G. Hopkins and M.J. Sewell (eds.), *Mechanics of Solids*. Oxford: Pergamon Press (1982) pp. 607–652.
10. M.M. Mehrabadi and S.C. Cowin, Initial planar deformation of dilatant granular materials. *J. Mech. Phys. Solids* 26 (1978) 269–284.
11. R. Butterfield and R.M. Harkness, The kinematics of Mohr-Coulomb materials. In: R.H.G. Parry (ed.), *Stress–Strain Behaviour of Soils*. Henley: Foulis (1972) pp. 220–281.
12. G. de Josselin de Jong, *Statics and Kinematics of the Failable Zone of a Granular Material*. Doctoral thesis. Delft: Uitgeverij Waltman (1959).
13. G. de Josselin de Jong, Mathematical elaboration of the double-sliding, free-rotating model. *Archs. Mech*. 29 (1977) 561–591.
14. G. de Josselin de Jong, Elasto-plastic version of the double-sliding model in undrained simple shear tests. *Geotechnique* 38 (1988) 533–555.
15. A.J.M. Spencer, Remarks on coaxiality in fully developed gravity flows of dry granular materials. In: N.A. Fleck and A.C.F. Cocks (eds.), *Mechanics of Granular and Porous Materials*. Dordrecht: Kluwer (1997) pp. 227–238.
16. A.J.M. Spencer and N.J. Bradley, Gravity flow of granular materials in contracting cylinders and tapered tubes. *Int. J. Eng. Sci*. 40 (2002) 1529–1552.
17. A.J.M. Spencer, Instability of steady flow of granular materials. *Acta Mech*. 64 (1986) 77–87.
18. D.G. Schaeffer, Instability in the evolution equations describing incompressible granular flow. *J. Diff. Eqns.* 66 (1987) 19–50.
19. D. Harris, Ill- and well-posed models of granular flow. *Acta Mech*. 146 (2001) 199–225.
20. D. Harris, Modelling mathematically the flow of granular materials. In: N.A. Fleck and A.C.F. Cocks (eds.), *Mechanics of Granular and Porous Materials*. Dordrecht: Kluwer (1997) pp. 239–250.
21. D. Harris, Discrete and continuum models in the mechanics of granular materials. In: R.P. Behringer, and J.T. Jenkins. (eds.), *Powders and Grains 97*. Rotterdam: A.A. Balkema (1997) pp. 247–250.
22. R. Jyotsna and K.K. Rao, A frictional-kinetic model for the flow of granular materials through a wedge-shaped hopper. *J. Fluid Mech*. 346 (1997) 239–270.
23. L.S. Mohan, P.R. Nott and K.K. Rao, Fully developed flow of coarse granular materials through a vertical channel. *Chem. Engng. Sci*. 52 (1997) 913–933.
24. S.B. Savage, Analyses of slow high-concentration flows of granular materials. *J. Fluid Mech*. 377 (1998) 1–26.
25. G.I. Tardos, S. McNamara and I. Talu, Slow and intermediate flow of a frictional bulk powder in the Couette geometry. *Powder Tech*. 131 (2003) 23–39.
26. S. Chapman and T.G. Cowling, *The Mathematical Theory of Non-Uniform Gases*. Cambridge: Cambridge University Press (1970) 423 pp.
27. W. Voigt, *Theoretische Studien über Elastizitätsverhältnisse der Kristalle*. Abh. Ges. Wiss., Gottingen. 34 (1887).
28. E. Cosserat and F. Cosserat, *Theorie des Corps Deformables*, Paris: A. Herman et Fils (1909) vi, p. 226.
29. A.P.S. Selvadurai, Bending of an infinite beam on a porous elastic medium. *Geotechnique* 23 (1973) 407–421.
30. E. Kröner (Ed.), *Mechanics of Generalized Continua, Proc. IUTAM Symposium*, Stuttgart and Freudenstadt. Berlin: Springer-Verlag (1968) 358 pp.
31. I. Vardoulakis and J. Sulem, *Bifurcation Analysis in Geomechanics*. London: Blackie Academic and Professional (1995) 462 pp.
32. H.B. Mühlhaus, Shear band analysis in granular materials by Cosserat theory. *Ing. Arch*. 56 (1986) 389–399.
33. J. Tejchman and W. Wu, Numerical study of patterning of shear bands in a Cosserat continuum. *Acta Mech*. 99 (1993) 61–74.
34. E. Bauer, Calibration of a comprehensive constitutive equation for granular materials. *Soils and Foundations* 36 (1996) 13–26.
35. J. Tejchman and E. Bauer, Numerical simulation of shear band formation with a polar hypoplastic constitutive model. *Computers and Geotechnics* 19 (1996) 221–244.
36. J. Tejchman and G. Gudehus, Shearing of a narrow granular layer with polar quantities. *Int. J. Numer. Anal. Meth. Geomech.* 25 (2001) 1–28.
37. L.S. Mohan, P.R. Nott and K.K. Rao, A frictional Cosserat model for the flow of granular materials through a vertical channel. *Acta Mech*. 138 (1999) 75–96.
38. L.S. Mohan, K.K. Rao and P.R. Nott, A frictional Cosserat model for the slow shearing of granular materials. *J. Fluid Mech*. 457 (2002) 377–409.

39. R.O. Davis and A.P.S. Selvadurai, *Plasticity and Geomechanics*. Cambridge: Cambridge University Press (2002), 287 pp.
40. C. Truesdell, Hypo-elasticity. *J. Rational Mech. Anal*. 4 (1955) 83–133, 1019–1020.
41. A.E. Green, Hypo-elasticity and Plasticity. *Proc. R. Soc. London A*. 234 (1956) 46–59.
42. A.E. Green, Hypo-elasticity and Plasticity II. *J. Rational Mech. Anal.* 5 (1956) 637–642.
43. C. Truesdell and W. Noll, *The Non-Linear Field Theories of Mechanics*. Handbuch der Physik, Vol. III/3 (S. Flugge, Ed.). Berlin: Springer-Verlag (1965) 602 pp.
44. W. Jaunzemis, *Continuum Mechanics*. New York: The Macmillan Co (1967) 604 pp.
45. D. Kolymbas, A novel constitutive law for soils, In: C.S. Desai (eds.), *Proceedings of the Second International Conference on Constitutive Laws for Engineering Materials*. Amsterdam: Elsevier (1987) pp. 319–326.
46. G. Gudehus, A comprehensive constitutive equation for granular materials. *Soils and Foundations* 36 (1996) 1–12.
47. W. Wu, *Hypoplasticity as a Mathematical Model for the Mechanical Behaviour of Granular Materials*. Publication Series of the Institute for Soil and Rock Mechanics, No. 129. Germany: University of Karlsruhe (1992).
48. W. Wu, E. Bauer and D. Kolymbas, Hypoplastic constitutive model with critical state for granular materials. *Mech. Mater.* 23 (1996) 45–69.
49. D. Kolymbas, Introduction to hypoplasticity. In: *Advances in Geotechnical Engineering and Tunnelling*, Vol. 1. Rotterdam: A.A. Balkema (2000) 94 pp.
50. W. Wu and D. Kolymbas, Hypoplasticity, then and now. In: D. Kolymbas (ed.), *Constitutive Modelling of Granular Materials*. Berlin: Springer Verlag (2000) pp. 57–105.
51. J.M. Hill and T.L. Katoanga, The velocity equations for dilatant granular flow and a new exact solution. *ZAMP* 48 (1997) 1–8.
52. J.M. Hill, Similarity 'hot-spot' solutions for a hypoplastic granular material. *Proc. R. Soc. London* A 456 (2000) 2653–2671.
53. J.M. Hill, Some symmetrical cavity problems for a hypoplastic granular material. *Q. J. Mech. Appl. Math.* 53 (2000) 111–135.
54. J.M. Hill and K.A. Williams, Dynamical uniaxial compaction of a hypoplastic granular material. *Mech. Mater.* 32 (2000) 679–691.
55. W. Wu and A. Niemunis, Failure criterion, flow rule and dissipation function derived from hypoplasticity. *Mech. Cohesive-Frict. Mater.* 1 (1996) 145–163.
56. P.-A. von Wolffersdorff, A hypoplastic relation for granular materials with a predefined limit state surface. *Mech. Cohesive-Frict. Mater.* 1 (1996) 251–271.
57. H. Matsuoka and T. Nakai, Stress-strain relationship of soil based on the SMP. In: Proceedings of Specialty Session 9, *9th International Conference on Soil Mechanics and Foundation Engineering*, Tokyo (1997) pp. 153–162.
58. A.J.M. Spencer, Double-shearing theory applied to instability and strain localization in granular materials. *J. Engng. Math*. 45 (2003) 55–74.
59. J.W. Rudnicki and J. Rice, Conditions for the localization of deformation in pressure sensitive dilatant materials. *J. Mech. Phys. Solids* 23 (1975) 371–394.
60. W. Huang and E. Bauer, Numerical investigations of shear localization in a micro-polar hypoplastic material. *Int. J. Numer. Anal. Meth. Geomech*. 27 (2003) 325–352.
61. S.C. Cowin and M. Satake (eds.), *Continuum Mechanical and Statistical Approaches in the Mechanics of Granular Materials*, Proc. U.S.-Japan Seminar, Sendai. Tokyo: Gakujutsu Bunken Fukyu-Kai (1978) 350 pp.
62. P. Vermeer and H.J. Luger (eds.), *Deformation and Failure of Granular Materials*. Proc. IUTAM Symposium, Delft. Rotterdam: A.A. Balkema (1982) 661 pp.
63. J.T. Jenkins and M. Satake (eds.), *Mechanics of Granular Materials. New Models and Constitutive Relations*. Proc. U.S./Japan Seminar, Ithaca, N.Y. Studies in Applied Mechanics, Vol.7. Amsterdam: Elsevier (1983) 364 pp.
64. M. Shahinpoor (ed.), *Advances in the Mechanics and Flow of Granular Materials*. Reston, VA: Gulf Publ. Co. (1983) 975 pp.
65. M. Satake (ed.), *Micromechanics of Granular Materials*. Proc. US-Japan Seminar, Sendai-Zao. Amsterdam: Elsevier (1988) 366 pp.
66. B.L. Keyfitz and M. Shearer (eds.), *Nonlinear Evolution Equations that Change Type*. Berlin: Springer Verlag (1991) 284 pp.

67. H. Shen, C.S. Campbell, M. Mehrabadi, C.S. Chang, and M. Satake (eds.), *Advances in Micromechanics of Granular Materials*. Proc. 2nd US/Japan Seminar, Potsdam. Amsterdam: Elsevier (1992) 462 pp.
68. M. Mehrabadi (ed.), *Mechanics of Granular Materials and Powder Systems*. New York: ASME (1992) 152 pp.
69. C.S. Chang (ed.), *Advances in Micromechanics of Granular Materials*. Amsterdam: Elsevier (1992) 462 pp.
70. D. Bideau and A. Hansen (eds.), *Disorder and Granular Media*. Random Materials and Processes Series. The Netherlands: North Holland (1993) 348 pp.
71. N.A. Fleck and A.F.C. Cocks (eds.), *IUTAM Symposium on Mechanics of Granular and Porous Materials*. Dordrecht: Kluwer (1997) 450 pp.
72. H.J. Herrmann, J.-P. Hovi and S. Luding (eds.), *Physics of Dry Granular Media*. Dordrecht: Kluwer (1998) 710 pp.
73. D.A. Drew, D.D. Joseph and S. Passman (eds.), *Particulate Flows. Processing and Rheology*. Berlin: Springer-Verlag (1998) 142 pp.
74. K.M. Golden, G.R. Grimmett, R.D. James, G.W. Milton and P.N. Sen (eds.), *Mathematics of Multi-Scale Materials*. Berlin: Springer-Verlag (1998) 280 pp.
75. P. Vermeer, S. Diebels, W. Ehlers, H.J. Herrmann, S. Luding and E. Ramm (eds.), *Continuous and Discontinuous Modelling of Cohesive-Frictional Materials*. Berlin: Springer-Verlag (2001) 307 pp.
76. T. Pöschel and S. Luding (eds.), *Granular Gases*. Berlin: Springer Verlag (2001) 457 pp.
77. G. Capriz, V.N. Ghionna and P. Giovine (eds.), *Modeling and Mechanics of Granular and Porous Materials*. Boston: Birkhauser (2002) 369 pp.
78. H. Hinrichsen and D.E. Wolf (eds.), *The Physics of Granular Media*. New York: John Wiley (2005) 364 pp.

Journal of Engineering Mathematics (2005) 52: 11–34
DOI 10.1007/s10665-004-6675-0

The incremental response of soils. An investigation using a discrete-element model

F. ALONSO-MARROQUÍN and H.J. HERRMANN
Institute of Computer Physics, University of Stuttgart, Pffafenwaldring 27, 70569 Stuttgart, Germany (fernando@ica1.uni-stuttgart.de)

Received 21 July 2004; accepted in revised form 19 November 2004

Abstract. The incremental stress-strain relation of dense packings of polygons is investigated by using molecular-dynamics simulations. The comparison of the simulation results to the continuous theories is performed using explicit expressions for the averaged stress and strain over a representative volume element. The discussion of the incremental response raises two important questions of soil deformation: Is the incrementally nonlinear theory appropriate to describe the soil mechanical response? Does a purely elastic regime exist in the deformation of granular materials? In both cases the answer will be "no". The question of stability is also discussed in terms of the Hill condition of stability for non-associated materials. It is contended that the incremental response of soils should be revisited from micromechanical considerations. A micromechanical approach assisted by discrete element simulations is briefly outlined.

Key words: elastoplasticity, granular materials, hypoplasticity, incremental response

1. Introduction

For many years the study of the mechanical behavior of soils was developed in the framework of linear elasticity [1, Chapter 1] and the Mohr-Coulomb failure criterion [2]. However, since the start of the development of the nonlinear constitutive relations in 1968 [3], a great variety of constitutive models describing different aspects of soils have been proposed [4]. A crucial question has been brought forward: What is the most appropriate constitutive model to interpret the experimental results, or to implement a finite-element code? Or more precisely, why is the constitutive relation I am using better than that one of the fellow in the next lab?

In the last years, the discrete-element approach has been used as a tool to investigate the mechanical response of soils at the grain level [5]. Several averaging procedures have been proposed to define the stress [6–8] and the strain tensor [9,10] in terms of the contact forces and displacements at the individual grains. These methods have been used to perform a direct calculation of the incremental stress-strain relation of assemblies of disks [11] and spheres [12], without any *a priori* hypothesis about the constitutive relation. Some of the results lead to the conclusion that the nonassociated elastoplasticity theory is sufficient to describe the observed incremental behavior [11]. However, some recent investigations using three-dimensional loading paths of complex loading histories seem to contradict these results [12,13]. Since the simple spherical geometries of the grains overestimate the role of rotations in realistic soils [13], it is interesting to evaluate the incremental response using arbitrarily shaped particles.

In this paper we investigate the incremental response in the quasistatic deformation of dense assemblies of polygonal particles. The comparison of the numerical simulations with the constitutive theories is performed by introducing the concept of *Representative Volume Element* (RVE). This volume is chosen the smear out the strong fluctuations of the stress and the

deformation in the granular assembly. In the averaging, each grain is regarded as a piece of continuum. By supposing that the stress and the strain of the grain are concentrated at the small regions of the contacts, we obtain expressions for the averaged stress and strain over the RVE, in terms of the contact forces, and the individual displacements and rotations of the grains. The details of this homogenization method are presented in Section 2. A short review of incremental, rate-independent stress-strain models is presented in Section 3. We emphasize particularly the classical Drucker-Prager elastoplastic models and the recently elaborated theory of hypoplasticity. The details of the particle model are presented in Section 4. The interparticle forces include elasticity, viscous damping and friction with the possibility of slip. The system is driven by applying stress-controlled tests on a rectangular framework consisting of four walls. Some loading programs will be implemented in Section 5, in order to deal with four basic questions on the incremental response of soils: (1) The existence of tensorial zones in the incremental response, (2) the validity of the superposition principle, (3) the existence of a finite elastic regime and (4) the question of stability according to the Hill condition. A micromechanical approach for soil deformation is outlined in the concluding remarks.

2. Homogenization

The aim of this section is to calculate the macromechanical quantities, the stress and strain tensors, from micromechanical variables of the granular assembly such as contact forces, rotations and displacements of individual grains.

A particular feature of granular materials is that both the stress and the deformation gradient are very concentrated in small regions around the contacts between the grains, so that they vary strongly over short distances. The standard homogenization procedure smears out these fluctuations by averaging these quantities over a RVE. The diameter d of the RVE must be such that $\delta \ll d \ll D$, where δ is the characteristic diameter of the particles and D is the characteristic length of the continuous variables.

We use this procedure here to obtain the averages of the stress and the strain tensors over a RVE in granular materials, which will allow us to compare the molecular dynamics simulations to the constitutive theories. We regard stress and strain to be continuously distributed

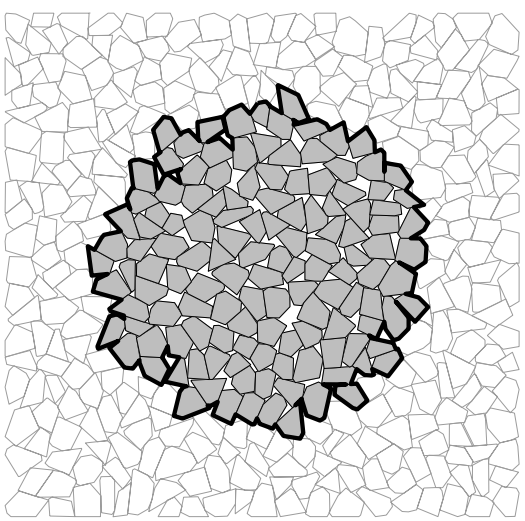

Figure 1. Representative volume element (RVE) used to calculate the incremental response.

through the grains, but concentrated at the contacts. It is important to note that this averaging procedure would not be appropriate to describe the structure of the chain forces or the shear band because typical variations of the stress correspond to few particle diameters. Different averaging procedures involving coarse-grained functions [8], or cutting the space in slide-shaped areas [10,14] allow to perform averages, and at the same time maintain these features.

We will calculate the averages around a point $\mathbf{x}_0$ of the granular sample taking a RVE calculated as follows: at the initial configuration, we select the grains whose centers of mass are less than d from $\mathbf{x}_0$. Then the RVE is taken as the volume V enclosed by the initial configuration of the grains; see Figure 1. The diameter d is taken such that the averaged quantities are not sensible to an increase of the diameter by one particle diameter.

2.1. Micromechanical stress

The Cauchy stress tensor is defined using the force acting on an area element situated on or within the grains. Let $\mathbf{f}$ be the force applied on a surface element a whose normal unit vector is $\mathbf{n}$. Then the stress is defined as the tensor satisfying [1, pp. 12–35]:

$$\sigma_{kj} n_k = \lim_{a \to 0} f_j / a, \tag{1}$$

where the Einstein summation convention is used. In absence of body forces, the equilibrium equations in every volume element lead to [1]:

$$\partial \sigma_{ij} / \partial x_i = 0. \tag{2}$$

We will calculate the average of the stress tensor $\bar{\sigma}$ over the RVE:

$$\bar{\sigma} = \frac{1}{V} \int_V \sigma \, \mathrm{d}V. \tag{3}$$

Since there is no stress in the voids of the granular media, the averaged stress can be written as the sum of integrals taken over the particles [7]

$$\bar{\sigma} = \frac{1}{V} \sum_{\alpha=1}^{N} \int_{V_\alpha} \sigma_{ij} \mathrm{d}V, \tag{4}$$

where V_α is the volume of the particle α and N is the number of particles of the RVE. By use of the identity

$$\frac{\partial (x_i \sigma_{kj})}{\partial x_k} = x_i \frac{\partial \sigma_{kj}}{\partial x_k} + \sigma_{ij}, \tag{5}$$

Equation (2), and the Gauss theorem, Equation (4) leads to [6]

$$\bar{\sigma}_{ij} = \frac{1}{V} \sum_{\alpha} \int_{V_\alpha} \frac{\partial (x_i \sigma_{kj})}{\partial x_k} \mathrm{d}V = \frac{1}{V} \sum_{\alpha} \int_{\partial V_\alpha} x_i \sigma_{kj} n_k \mathrm{d}a. \tag{6}$$

The right-hand side is the sum over the surface integrals of each grain. Further, ∂V_α represents the surface of the grain α and $\mathbf{n}$ is the unit normal vector to the surface element da.

An important feature of granular materials is that the stress acting on each grain boundary is concentrated in the small regions near to the contact points. Then we can use

the definition given in (1) to express this stress on particle α in terms of the contact forces by introducing Dirac delta functions:

$$\sigma_{kj} n_k = \sum_{\beta=1}^{N_\alpha} f_j^{\alpha\beta} \delta(\mathbf{x} - \mathbf{x}^{\alpha\beta}), \tag{7}$$

where $\mathbf{x}^{\alpha\beta}$ and $\mathbf{f}^{\alpha\beta}$ are the position and the force at the contact β, and N_α is the number of contacts of the particle α. Inserting (7) into (6), we obtain

$$\bar{\sigma}_{ij} = \frac{1}{V} \sum_{\alpha\beta} x_i^{\alpha\beta} f_j^{\alpha\beta}. \tag{8}$$

Now we decompose $\mathbf{x}^{\alpha\beta} = \mathbf{x}^{\alpha} + \boldsymbol{\ell}^{\alpha\beta}$, where $\mathbf{x}^{\alpha}$ is the position of the center of mass and $\boldsymbol{\ell}^{\alpha\beta}$ is the branch vector, connecting the center of mass of the particle to the point of application of the contact force. Imposing this decomposition in (8), and using the equilibrium equations at each particle $\sum_\beta \mathbf{f}^{\alpha\beta} = 0$, we have

$$\bar{\sigma}_{ij} = \frac{1}{V} \sum_{\alpha\beta} \ell_i^{\alpha\beta} f_j^{\alpha\beta}. \tag{9}$$

From the equilibrium equations of the torques $\sum_\beta (\ell_i^{\alpha\beta} f_j^{\alpha\beta} - \ell_j^{\alpha\beta} f_i^{\alpha\beta}) = 0$ one obtains that this tensor is symmetric, *i.e.,*

$$\bar{\sigma}_{ij} - \bar{\sigma}_{ji} = 0. \tag{10}$$

Then, the eigenvalues of this matrix are always real. This property leads to some simplifications, as we will see later.

2.2. Micromechanical strain

In elasticity theory, the strain tensor is defined as the symmetric part of the average of the displacement gradient with respect to the equilibrium configuration of the assembly. Using the law of conservation of energy, one can define the stress–strain relation in this theory [1, Section 2.2]. In granular materials, it is not possible to define the strain in this sense, because any loading involves a certain amount of plastic deformation at the contacts, so that it is not possible to define the initial configuration to calculate the strain. Nevertheless, one can define a strain tensor in the incremental sense. This is defined as the average of the displacement tensor taken from the deformation during a certain time interval.

At the micromechanical level, the deformation of the granular materials is given by a displacement field $\mathbf{u} = \mathbf{r}' - \mathbf{r}$ at each point of the assembly. Here $\mathbf{r}$ and $\mathbf{r}'$ are the positions of a material point before and after deformation. The average of the strain and rotational tensors are defined as [15]:

$$\bar{\epsilon} = \frac{1}{2}(F + F^T), \tag{11}$$

$$\bar{\omega} = \frac{1}{2}(F - F^T). \tag{12}$$

Here F^T is the transpose of the deformation gradient F, which is defined as [6]

$$F_{ij} = \frac{1}{V} \int_V \frac{\partial u_i}{\partial x_j} \mathrm{d}V. \tag{13}$$

Using the Gauss theorem, we transform it into an integral over the surface of the RVE

$$F_{ij} = \frac{1}{V} \int_{\partial V} u_i n_j \mathrm{d}a, \tag{14}$$

where ∂V is the boundary of the volume element. We express this as the sum over the boundary particles of the RVE

$$F_{ij} = \frac{1}{V} \sum_{\alpha=1}^{N_b} \int_{\partial V_\alpha} u_i n_j \mathrm{d}a, \tag{15}$$

where N_b is the number of boundary particles. It is now convenient to make some approximations. First, the displacements of the grains during deformation can be considered rigid, except for small deformations near to the contacts, which can be neglected. Then, if the displacements are small in comparison with the size of the particles, we can write the displacement of the material points inside particle α as:

$$u_i(\mathbf{x}) \approx \Delta x_i^\alpha + e_{ijk} \Delta \phi_j^\alpha (x_k - x_k^\alpha), \tag{16}$$

where $\Delta \mathbf{x}^\alpha$, $\Delta \boldsymbol{\phi}^\alpha$ and $\mathbf{x}^\alpha$ are displacement, rotation and center of mass of the particle α which contains the material point $\mathbf{x}$, and e_{ijk} is the antisymmetric unit tensor. Setting a parameterization for each surface of the boundary grains over the RVE, we can calculate the deformation gradient explicitly in terms of grain rotations and displacements by substituting (16) in (15).

In the particular case of a bidimensional assembly of polygons, the boundary of the RVE is given by a graph $\{\mathbf{x}_1, \mathbf{x}_2, \ldots, \mathbf{x}_{N_b+1} = \mathbf{x}_1\}$ consisting of all the edges belonging to the external contour of the RVE, as shown in Figure 1. In this case, Equation (15) can be transformed into a sum of integrals over the segments of this contour.

$$F_{ij} = \frac{1}{V} \sum_{\beta=1}^{N_b} \int_{x_\beta}^{x_{\beta+1}} \left[\Delta x_i^\beta + e_{ik} \Delta \phi^\beta (x_k - x_k^\beta) \right] n_j^\beta \mathrm{d}s, \tag{17}$$

where $e_{ik} \equiv e_{i3k}$ and the unit vector $\mathbf{n}^\beta$ is perpendicular to the segment $\overrightarrow{x^\beta x^{\beta+1}}$. Here β corresponds to the index of the boundary segment; $\Delta \mathbf{x}^\beta$, $\Delta \boldsymbol{\phi}^\beta$ and $\mathbf{x}^\beta$ are displacement, rotation and center of mass of the particle which contains this segment. Finally, by using the parameterization $\mathbf{x} = \mathbf{x}^\beta + s(\mathbf{x}^{\beta+1} - \mathbf{x}^\beta)$, where $(0 < s < 1)$, we can integrate (17) to obtain

$$F_{ij} = \frac{1}{V} \sum_{\beta} \left(\Delta x_i^\beta + e_{ik} \Delta \phi^\beta \ell_k^\beta \right) N_j^\beta, \tag{18}$$

where $N_j^\beta = e_{j,k} \left(x_k^{\beta+1} - x_k^\beta \right)$ and $\boldsymbol{\ell} = (\mathbf{x}^{\beta+1} - \mathbf{x}^\beta)/2 - \mathbf{x}^\alpha$. We can calculate the stress tensor by taking the symmetric part of this tensor using Equation (11). Contrary to the strain tensor calculated for spherical particles [8,16], the individual rotations of the particles are included in the calculation of this tensor. This is borne out by the fact that for nonspherical particles the branch vector is not perpendicular to the contact normal vector, so that $e_{ik} \ell_k^\beta N_j^\beta \neq 0$.

3. Incremental theory

Since the stress and the strain are symmetric tensors, it is advantageous to simplify the notation by defining these quantities as six-dimensional vectors:

$$\tilde{\sigma} = \begin{bmatrix} \bar{\sigma}_{11} \\ \bar{\sigma}_{22} \\ \bar{\sigma}_{33} \\ \sqrt{2}\bar{\sigma}_{23} \\ \sqrt{2}\bar{\sigma}_{31} \\ \sqrt{2}\bar{\sigma}_{13} \end{bmatrix} \quad \text{and} \quad \tilde{\epsilon} = \begin{bmatrix} \bar{\epsilon}_{11} \\ \bar{\epsilon}_{22} \\ \bar{\epsilon}_{33} \\ \sqrt{2}\bar{\epsilon}_{23} \\ \sqrt{2}\bar{\epsilon}_{31} \\ \sqrt{2}\bar{\epsilon}_{13} \end{bmatrix}. \tag{19}$$

The coefficient $\sqrt{2}$ allows us to preserve the metric in this transformation: $\tilde{\sigma}_k\tilde{\sigma}_k = \bar{\sigma}_{ij}\bar{\sigma}_{ij}$. The relation between these two vectors will be established in the general context of the rate-independent incremental constitutive relations. We will focus on two particular theoretical developments: the theory of hypoplasticity and the elastoplastic models. The similarities and differences of both formulations are presented in the framework of the incremental theory that follows.

3.1. General framework

In principle, the mechanical response of granular materials can be described by a functional dependence of the stress $\tilde{\sigma}(t)$ at time t on the strain history $\{\tilde{\epsilon}(t')\}_{0<t'<t}$. However, the mathematical description of this dependence turns out to be very complicated due to the nonlinearity and irreversible behavior of these materials. An incremental relation, relating the incremental stress $\mathrm{d}\tilde{\sigma}(t) = \sigma'(t)\mathrm{d}t$ to the incremental strain $\mathrm{d}\tilde{\epsilon}(t) = \epsilon'(t)\mathrm{d}t$ and some internal variables κ that account for the deformation history, enable us to avoid these mathematical difficulties [17]. This incremental scheme is also useful for solving geotechnical problems, since the finite-element codes require that the constitutive relation be expressed incrementally.

Due to the large number of existing incremental relations, the necessity of a unified theoretical framework has been pointed out as an essential necessity to classify all the existing models [18]. In general, the incremental stress is related to the incremental strain as follows:

$$\mathcal{F}_\kappa(\mathrm{d}\tilde{\epsilon}, \mathrm{d}\tilde{\sigma}, \mathrm{d}t) = 0. \tag{20}$$

Let us look at the special case where there is no rate-dependence in the constitutive relation. This means that this relation is not influenced by the time required during any loading tests, as corresponds to the quasistatic approximation. In this case $\mathcal{F}$ is invariant with respect to $\mathrm{d}t$, and (20) can be reduced to:

$$\mathrm{d}\tilde{\epsilon} = \mathcal{G}_\kappa(\mathrm{d}\tilde{\sigma}) \tag{21}$$

In particular, the rate-independent condition implies that multiplying the loading time by a scalar λ does not affect the incremental stress-strain relation:

$$\forall\lambda, \quad \mathcal{G}_\kappa(\lambda\mathrm{d}\tilde{\sigma}) = \lambda\mathcal{G}_\kappa(\mathrm{d}\tilde{\sigma}) \tag{22}$$

The significance of this equation is that $\mathcal{G}_\kappa$ is an homogeneous function of degree one. In this case, the application of the Euler identity shows that (21) leads to

$$\mathrm{d}\tilde{\epsilon} = M_\kappa(\hat{\sigma})\mathrm{d}\tilde{\sigma}, \tag{23}$$

where $M_\kappa = \partial \mathcal{G}_\kappa / \partial(\mathrm{d}\tilde{\sigma})$ and $\hat{\sigma}$ is the unitary vector defining the direction of the incremental stress

$$\hat{\sigma} = \frac{\mathrm{d}\tilde{\sigma}}{|\mathrm{d}\tilde{\sigma}|}. \tag{24}$$

Equation (23) represents the general expression for the rate-independent constitutive relation. In order to determine the dependence of M on $\hat{\sigma}$, one can either perform experiments by taking different loading directions, or postulate explicit expressions based on a theoretical framework. The first approach will be considered in the Subsection 5.2, and the discussion about some existing theoretical models will be presented in the following.

3.2. Elastoplastic models

The classical elastoplasticity theory was established by Drucker and Prager in the context if metal plasticity [19]. Some extensions have been developed to describe sand, clays, rocks, concrete, etc. [2,20]. Here we present a short review of these developments in soil mechanics.

When a granular sample, subjected to a confining pressure, is loaded in the axial direction, it displays a typical stress-strain response as shown in the left part of Figure 2. A continuous decrease of the stiffness (*i.e.*, the slope of the stress-strain curve) is observed during loading. If the sample is unloaded, an abrupt increase in the stiffness is observed, leaving an irreversible deformation. One observes that, if the stress is changed around some region below σ_A, which is called the *yield point*, the deformation is almost linear and reversible. The first postulate of the elastoplasticity theory establishes a stress region immediately below the yield point where only elastic deformations are possible.

Postulate 1: For each stage of loading there exists a yield surface which encloses a finite region in the stress space where only reversible deformations are possible.

The simple Mohr-Coulomb model assumes that the onset of plastic deformation occurs at failure [2]. However, it has been experimentally shown that plastic deformation develops before failure [21]. In order to provide a consistent description of these experimental results with the elastoplasticity theory, it is necessary to assume that the yield function changes with the deformation process [21]. This condition is schematically shown in Figure 2. Let us assume that the sample is loaded until it reaches the stress σ_A upon which it is slightly unloaded. If the sample is reloaded, it is able to recover the same stress-strain relation of the monotonic loading once it reaches the yield point σ_A again. If one increases the load to the stress σ_B, a new elastic regime can be observed after a loading reversal. In the elastoplasticity

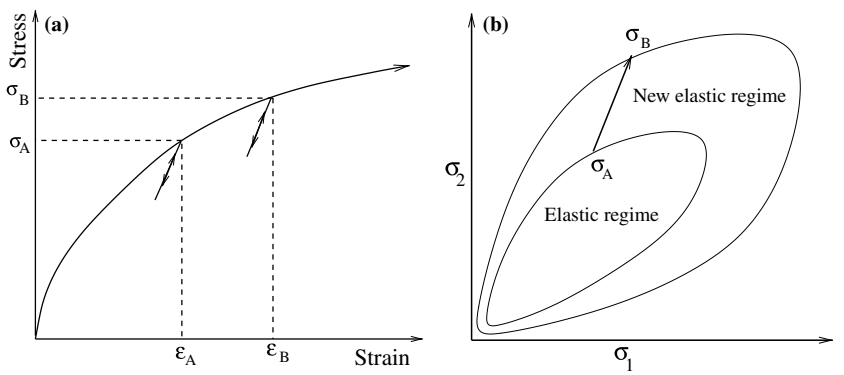

Figure 2. Evolution of the elastic regime (a) stress-strain relation (b) elastic regime in the stress space.

theory, this result is interpreted by assuming that the elastic regime is expanded to a new stress region below the yield point σ_B.

Postulate 2: The yield function remains when the deformations take place inside of the elastic regime, and it changes as the plastic deformation evolves.

The transition from the elastic to the elastoplastic response is extrapolated for more general deformations. Part (b) of Figure 2 shows the evolution of the elastic region when the yield point moves in the stress space from $\tilde{\sigma_A}$ to $\tilde{\sigma_B}$. The essential goal in the elastoplasticity theory is to find the correct description of the evolution of the elastic regime with the deformation, which is called the *hardening law*.

We will finally introduce the third basic assumption from elastoplasticity theory:

Postulate 3: The strain can be separated in an elastic (recoverable) and a plastic (unrecoverable) component:

$$\mathrm{d}\tilde{\epsilon} = \mathrm{d}\tilde{\epsilon}^e + \mathrm{d}\tilde{\epsilon}^p, \tag{25}$$

The incremental elastic strain is linked to the incremental stress by introducing an elastic tensor as

$$\mathrm{d}\tilde{\sigma} = D(\tilde{\sigma})\mathrm{d}\tilde{\epsilon}^e. \tag{26}$$

To calculate the incremental plastic strain, we introduce the *yield surface* as

$$f(\sigma, \kappa) = 0, \tag{27}$$

where κ is introduced as an internal variable, which describes the evolution of the elastic regime with the deformation. From experimental evidence, it has been shown that this variable can be taken as a function of the cumulative plastic strain ϵ^p given by [2,20]

$$\epsilon^p \equiv \int_0^t \sqrt{\mathrm{d}\epsilon_k \mathrm{d}\epsilon_k}\mathrm{d}t \tag{28}$$

When the stress state reaches the yield surface, the plastic deformation evolves. This is assumed to be derived from a scalar function of the stress as follows:

$$\mathrm{d}\epsilon_j^p = \Lambda \frac{\partial g}{\partial \sigma_j}, \tag{29}$$

where g is the so-called *plastic potential* function. Following the Drucker-Prager postulates we can show that $g = f$ [19]. However, a considerable amount of experimental evidence has shown that in soils the plastic deformation is not perpendicular to the yield surfaces [22]. It is necessary to introduce this plastic potential to extend the Drucker-Prager models to the so-called *non-associated* models.

The parameter Λ of (29) can be obtained from the so-called *consistence condition*. This condition comes from the second postulate, which establishes that, after the movement of the stress state from $\tilde{\sigma_A}$ to $\tilde{\sigma_B} = \tilde{\sigma_A} + \tilde{\mathrm{d}\sigma}$, the elastic regime must be expanded so that $\mathrm{d}f = 0$, as shown in Part (b) of Figure 2. Using the chain rule one obtains:

$$\mathrm{d}f = \frac{\partial f}{\partial \sigma_i}\mathrm{d}\sigma_i + \frac{\partial f}{\partial \kappa}\frac{\partial \kappa}{\partial \epsilon_j^p}\mathrm{d}\epsilon_j^p = 0. \tag{30}$$

Inserting (29) into (30), we obtain the parameter Λ, *viz.*

$$\Lambda = -\left(\frac{\partial f}{\partial \kappa}\frac{\partial \kappa}{\partial \epsilon_j^p}\frac{\partial g}{\partial \sigma_j}\right)^{-1}\frac{\partial f}{\partial \sigma_i}\mathrm{d}\sigma_i. \tag{31}$$

We define the vectors $N_i^y = \partial f/\partial\sigma_i$ and $N_i^f = \partial g/\partial\sigma_i$ and the unit vectors $\hat{\phi} = \mathbf{N}^y/|\mathbf{N}^y|$ and $\hat{\psi} = \mathbf{N}^f/|\mathbf{N}^f|$ as the *flow direction* and the *yield direction*. In addition, the *plastic modulus* is defined as

$$h = -\frac{1}{|\mathbf{N}^y||\mathbf{N}^f|}\frac{\partial f}{\partial\kappa}\frac{\partial\kappa}{\partial\epsilon_i^p}\frac{\partial g}{\partial\sigma_i}. \tag{32}$$

Substituting (31) in (29) and using (32), we obtain:

$$\mathrm{d}\tilde{\epsilon}^p = \frac{1}{h}\hat{\phi}\cdot\mathrm{d}\tilde{\sigma}\ \ \hat{\psi}. \tag{33}$$

Note that this equation has been calculated in the case where the stress increment takes place outside the yield surface. If the stress increment occurs inside the yield surface, the second Drucker-Prager postulate establishes that $\mathrm{d}\tilde{\epsilon}^p = 0$. Thus, the generalization of (33) is given by

$$\mathrm{d}\tilde{\epsilon}^p = \frac{1}{h}\langle\hat{\phi}\cdot\mathrm{d}\tilde{\sigma}\rangle\ \ \hat{\psi}, \tag{34}$$

where $\langle x\rangle = x$ when $x > 0$ and $\langle x\rangle = 0$ otherwise. Finally, the total strain response can be obtained from (25) and (34):

$$\mathrm{d}\tilde{\epsilon} = D^{-1}(\tilde{\sigma})\mathrm{d}\tilde{\sigma} + \frac{1}{h}\langle\hat{\phi}\cdot\mathrm{d}\tilde{\sigma}\rangle\ \ \hat{\psi}. \tag{35}$$

From this equation one can distinguish two zones in the incremental stress space where the incremental relation is linear. They are the so-called tensorial zones defined by Darve and Laouafa [17]. The existence of two tensorial zones and the continuity of the incremental response at the boundary confirm that these two zones are essential features of the elastoplastic models.

Although the elastoplasticity theory has been proved to work well for monotonically increasing loading, it shows some deficiencies in the description of complex loading histories [23, pp. 230–262]. There is also an extensive body of experimental evidence that shows that the elastic regime is extremely small and that the transition from elastic to an elastoplastic response is not as sharp as the theory predicts [24].

The *bounding surface models* have been introduced to generalize the classical elastoplastic concepts [25]. Apart from the critical-state line, these models introduce the so-called bounding surface in the stress space. For any given stress state within the surface, a proper mapping rule associates a corresponding *image* stress point on this surface. A measure of the distance between the actual and the image stress points is used to specify the plastic modulus in terms of a plastic modulus at the image stress state. Besides the versatility of this theory to describe a wide range of materials, it has the advantage that the elastic regime can be considered as vanishingly small, so that this model can be used to give a realistic description of unbounded granular soils. In the authors' opinion, the most striking aspect of the bounding-surface theory with vanishing elastic range is that it establishes a convergence point for two different approaches of constitutive modeling: the elastoplastic approaches originated from the Drucker-Prager theory, and the more recently developed hypoplastic theories.

3.3. Hypoplastic models

In recent years, an alternative approach for modeling soil behavior has been proposed, which departs from the framework of the elastoplasticity theory [26–28]. The distinctive features of this approach are:

– *The absence of the decomposition of strain in plastic and elastic components.*
– *The statement of a nonlinear dependence of the incremental response with the strain rate directions.*

The most general expression has been provided by the so-called second-order incremental nonlinear models [27]. A particular class of these models which has received special attention in recent times is provided by the theory of hypoplasticity [26,28]. A general outline of this theory was proposed by Kolymbas [26], leading to different formulations, such as the K-hypoplasticity developed in Karlsruhe [29], and the CLoE-hypoplasticity originated in Grenoble [28]. In hypoplasticity, the most general constitutive equation takes the following form:

$$\mathrm{d}\tilde{\sigma} = L(\tilde{\sigma}, v)\mathrm{d}\tilde{\epsilon} + \tilde{N}(\tilde{\sigma}, v)|\mathrm{d}\tilde{\epsilon}|, \tag{36}$$

where L is a second-order tensor and $\tilde{N}$ is a vector, both depending on the stress $\tilde{\sigma}$ and the void ratio v. Hypoplastic equations provide a simplified description of loose and dense unbounded granular materials. A reduced number of parameters are introduced, which are very easy to calibrate [30].

In the theory of hypoplasticity, the stress-strain relation is established by means of an incremental nonlinear relation without any recourse to yield or boundary surfaces. This nonlinearity is reflected in the fact that the relation between the incremental stress and the incremental strain given in (36) is always nonlinear. The incremental nonlinearity of the granular materials is still under discussion. Indeed, an important feature of the incremental nonlinear constitutive models is that they break away from the superposition principle:

$$\mathrm{d}\tilde{\sigma}(\mathrm{d}\tilde{\epsilon}_1 + \mathrm{d}\tilde{\epsilon}_2) \neq \mathrm{d}\tilde{\sigma}(\mathrm{d}\tilde{\epsilon}_1) + \mathrm{d}\tilde{\sigma}(\mathrm{d}\tilde{\epsilon}_2), \tag{37}$$

which is equivalent to:

$$\mathrm{d}\tilde{\epsilon}(\mathrm{d}\tilde{\sigma}_1 + \mathrm{d}\tilde{\sigma}_2) \neq \mathrm{d}\tilde{\epsilon}(\mathrm{d}\tilde{\sigma}_1) + \mathrm{d}\tilde{\epsilon}(\mathrm{d}\tilde{\sigma}_2) \tag{38}$$

An important consequence of this feature is addressed by Kolymbas [31, pp. 213–223] and Darve et al. [27]. They consider two stress paths; the first one is smooth and the second results from the superposition of small deviations as shown in Figure 3. The superposition principle establishes that the strain response of the stair-like path converges to the response of the proportional loading in the limit of arbitrarily small deviations. More precisely, the strain deviations $\Delta\epsilon$ and the steps of the stress increments $\Delta\sigma$ satisfy $\lim_{\Delta\sigma\to 0}\Delta\epsilon = 0$. For the hypoplastic equations, and in general for the incremental nonlinear models, this condition is never satisfied. For incremental relations with tensorial zones, this principle is satisfied whenever the increments take place inside one of these tensorial zones. It should be added that there is no experimental evidence disproving or confirming this rather questionable superposition principle.

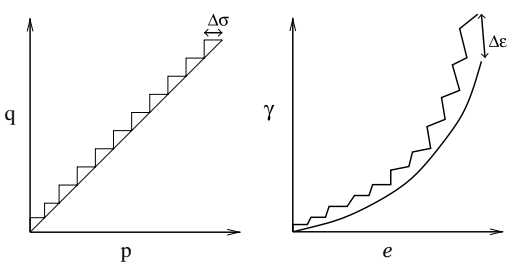

Figure 3. Smooth and stair-like stress paths and corresponding strain responses. p and q represent the pressure and the deviatoric stress. e and γ are the volumetric and deviatoric strain components.

4. Discrete model

We present here a two-dimensional discrete-element model which will be used to investigate the incremental response of granular materials. This model consists of randomly generated convex polygons, which interact via contact forces. There are some limitations in the use of such a two-dimensional code to model physical phenomena that are three-dimensional in nature. These limitations have to be kept in mind in the interpretation of the results and its comparison with the experimental data. In order to give a three-dimensional picture of this model, one can consider the polygons as a collection of bricks with randomly-shaped polygonal basis. Alternatively, one could consider the polygons as three-dimensional grains whose centers of mass all move in the same plane. In the authors' opinion, it is more sensible to consider this model as an idealized granular material that can be used to check the constitutive models.

The details of the particle generation, the contact forces, the boundary conditions and the molecular-dynamics simulations are presented in this section.

4.1. Generation of polygons

The polygons representing the particles in this model are generated by using the method of Voronoi tessellation [32]. This method is schematically shown in Figure 4. First, a regular square lattice of side ℓ is created. Then, we choose a random point in each cell of the rectangular grid. Subsequently, each polygon is constructed by assigning to each point that part of the plane that is nearer to it than to any other point. The details of the construction of the Voronoi cells can be found in the literature [33, 34].

By use of the Euler theorem, it has been shown analytically that the mean number of edges of this Voronoi construction must be 6 [34, pp. 295–296]. The number of edges of the polygons is distributed between 4 and 8 for 98·7% of the polygons. The orientational distribution of edges is isotropic, and the distribution of areas of polygons is symmetric around its mean value ℓ^2. The probabilistic distribution of areas follows approximately a Gaussian distribution with variance of $0{\cdot}36\ell^2$.

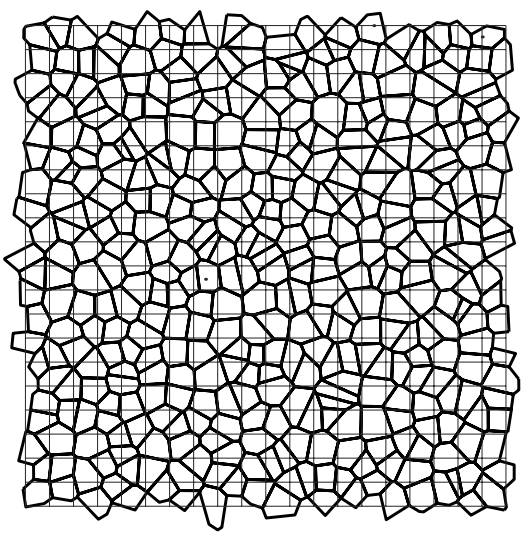

Figure 4. Voronoi construction used to generate the convex polygons. The dots indicate the point used in the tessellation. Periodic boundary conditions were used.

4.2. Contact forces

In order to calculate the forces, we assume that all the polygons have the same thickness L. The force between two polygons is written as $\mathbf{F}=\mathbf{f}L$ and the mass of the polygons is $M=mL$. In reality, when two elastic bodies come into contact, they have a slight deformation in the contact region. In the calculation of the contact force we assume that the polygons are rigid, but we allow them to overlap. Then, we calculate the force from this virtual overlap.

The first step towards the calculation of the contact force is the definition of the line representing the flattened contact surface between the two bodies in contact. This is defined from the contact points resulting from the intersection of the edges of the overlapping polygons. In most cases, we have two contact points, as shown in the left part of Figure 5. In such a case, the contact line is defined by the vector $\mathbf{C}=\overrightarrow{C_1C_2}$ connecting these two intersection points. In some pathological cases, the intersection of the polygons leads to four or six contact points. In these cases, we define the contact line by the vector $\mathbf{C}=\overrightarrow{C_1C_2}+\overrightarrow{C_3C_4}$ or $\mathbf{C}=\overrightarrow{C_1C_2}+\overrightarrow{C_3C_4}+\overrightarrow{C_5C_6}$, respectively. This choice guarantees a continuous change of the contact line, and therefore of the contact forces, during the evolution of the contact.

The contact force is separated as $\mathbf{f}^c=\mathbf{f}^e+\mathbf{f}^v$, where $\mathbf{f}^e$ and $\mathbf{f}^v$ are the elastic and viscous contribution. The elastic part of the contact force is decomposed as $\mathbf{f^e}=f_n^e\hat{n}^c+f_t^e\hat{t}^c$. The calculation of these components is explained below. The unit tangential vector is defined as $\hat{t}^c=\mathbf{C}/|\mathbf{C}|$, and the normal unit vector $\hat{n}^c$ is taken perpendicular to $\mathbf{C}$. The point of application of the contact force is taken as the center of mass of the overlapping polygons.

As opposed to the Hertz theory for round contacts, there is no exact way to calculate the normal force between interacting polygons. An alternative method has been proposed in order to model this force [35]. The normal elastic force is given by $f_n^e=-k_nA/L_c$, where k_n is the normal stiffness, A is the overlapping area and L_c is a characteristic length of the polygon pair. Our choice of L_c is $1/2(1/R_i+1/R_j)$ where R_i and R_j are the radii of the circles of the same area as the polygons. This normalization is necessary to be consistent in the units of force [32].

In order to model the quasistatic friction force, we calculate the elastic tangential force using an extension of the method proposed by Cundall-Strack [5]. An elastic force $f_t^e=-k_t\Delta x_t$ proportional to the elastic displacement is included at each contact, where k_t is the tangential stiffness. The elastic displacement Δx_t is calculated as the time integral of the tangential velocity of the contact during the time when the elastic condition $|f_t^e|<\mu f_n^e$ is satisfied. The sliding condition is imposed, keeping this force constant when $|f_t^e|=\mu f_n^e$. The

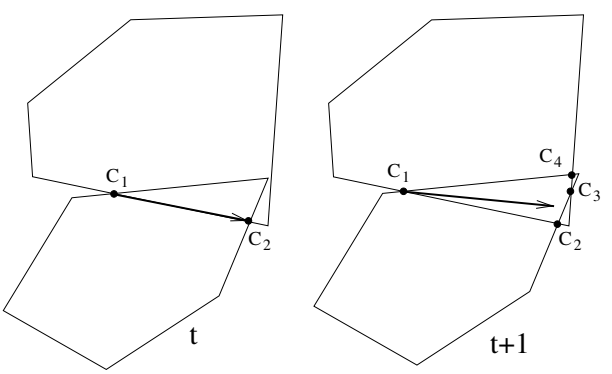

Figure 5. Contact points C_i before (left) and after the formation of a pathological contact (right). The vector denotes the contact line; t represents the time step.

straightforward calculation of this elastic displacement is given by the time integral starting at the beginning of the contact:

$$\Delta x_t^e = \int_0^t v_t^c(t')\Theta(\mu f_n^e - |f_t^e|)\mathrm{d}t', \tag{39}$$

where Θ is the Heaviside step function and $\mathbf{v}_t^c$ denotes the tangential component of the relative velocity $\mathbf{v}^c$ at the contact:

$$\mathbf{v}^c = \mathbf{v}_i - \mathbf{v}_j + \boldsymbol{\omega}_i \times \boldsymbol{\ell}_i - \boldsymbol{\omega}_j \times \boldsymbol{\ell}_j. \tag{40}$$

Here $\mathbf{v}_i$ is the linear velocity and $\boldsymbol{\omega}_i$ is the angular velocity of the particles in contact. The branch vector $\boldsymbol{\ell}_i$ connects the center of mass of particle i with the point of application of the contact force.

Damping forces are included in order to allow for rapid relaxation during the preparation of the sample, and to reduce the acoustic waves produced during the loading. These forces are calculated as

$$\mathbf{f}_v^c = -m(\gamma_n v_n^c \hat{n}^c + \gamma_t v_t^c \hat{t}^c), \tag{41}$$

$m = (1/m_i + 1/m_j)^{-1}$ being the effective mass of the polygons in contact; $\hat{n}^c$ and $\hat{t}^c$ are the normal and tangential unit vectors defined before, and γ_n and γ_t are the coefficients of viscosity. These forces introduce time-dependent effects during the cyclic loading. However, we will show that these effects can be arbitrarily reduced by increasing the loading time, which corresponds to the quasistatic approximation.

4.3. Molecular-dynamics simulation

The evolution of the position $\mathbf{x}_i$ and the orientation φ_i of the ith polygon is governed by the equations of motion:

$$\begin{aligned} m_i \ddot{\mathbf{x}}_i &= \sum_c \mathbf{f}_i^c + \sum_b \mathbf{f}_i^b, \\ I_i \ddot{\varphi}_i &= \sum_c \boldsymbol{\ell}_i^c \times \mathbf{f}_\mathbf{i}^\mathbf{c} + \sum_b \boldsymbol{\ell}_i^b \times \mathbf{f}_i^b. \end{aligned} \tag{42}$$

Here m_i and I_i are the mass and moment of inertia of the polygon i. The first summation goes over all particles in contact with this polygon. According to the previous section, these forces $\mathbf{f}^\mathbf{c}$ are given by

$$\mathbf{f}^c = -(k_n A/L_c + \gamma_n m v_n^c)\mathbf{n}^c - (\Delta x_t^c + \gamma_t m v_t^c)\mathbf{t}^c, \tag{43}$$

The second summation on the right hand of (42) goes over all the vertices of the polygons in contact with the walls. This interaction is modeled by using a simple visco-elastic force. First, we allow the polygons to penetrate the walls. Then, for each vertex of the polygon α inside of the walls we include a force

$$\mathbf{f}^b = -k_n \delta \mathbf{n} - \gamma_b m_\alpha \mathbf{v}^b, \tag{44}$$

where δ is the penetration length of the vertex, $\mathbf{n}$ is the unit normal vector to the wall, and $\mathbf{v}^b$ is the relative velocity of the vertex with respect to the wall.

We use a fifth-order Gear predictor-corrector method for solving the equation of motion [36, pp. 340–342]. This algorithm consists of three steps. The first step predicts position and

velocity of the particles by means of a Taylor expansion. The second step calculates the forces as a function of the predicted positions and velocities. The third step corrects the positions and velocities in order to optimize the stability of the algorithm. This method is much more efficient than the simple Euler approach or the Runge-Kutta method, especially for problems where very high accuracy is a requirement.

The parameters of the molecular-dynamics simulations were adjusted according to the following criteria: (1) guarantee the stability of the numerical solution, (2) optimize the time of the calculation, and (3) provide a reasonable agreement with the experimental data.

There are many parameters in the molecular-dynamics algorithm. Before choosing them, it is convenient to make a dimensional analysis. In this way, we can maintain the scale invariance of the model and reduce the parameters to a minimum of dimensionless constants. First, we introduce the following characteristic times of the simulations: the loading time t_0, the relaxation times $t_n = 1/\gamma_n$, $t_t = 1/\gamma_t$, $t_b = 1/\gamma_b$ and the characteristic period of oscillation $t_s = \sqrt{\rho \ell^2 / k_n}$ of the normal contact.

Using the Buckingham Pi theorem [37], one can show that the strain response, or any other dimensionless variable measuring the response of the assembly during loading, depends only on the following dimensionless parameters: $\alpha_1 = t_n/t_s$, $\alpha_2 = t_t/t_s$, $\alpha_3 = t_b/t_s$, $\alpha_4 = t_0/t_s$, the ratio $\zeta = k_t/k_n$ between the stiffnesses, the friction coefficient μ and the ratio σ_i/k_n between the stresses applied on the walls and the normal stiffness.

The variables α_i will be called *control parameters*. They are chosen in order to satisfy the quasistatic approximation, *i.e.*, the response of the system does not depend on the loading time, but a change of these parameters within this limit does not affect the strain response. Parameter values $\alpha_2 = 0{\cdot}1$ and $\alpha_2 = 0{\cdot}5$ were taken large enough to have a high dissipation, but not too large to keep the numerical stability of the method. The value $\alpha_3 = 0{\cdot}001$ is chosen by optimizing the time of consolidation of the sample in the Subsection 4.4. The ratio $\alpha_4 = t_0/t_s = 10{,}000$ was chosen large enough in order to avoid rate-dependence in the strain response, corresponding to the quasistatic approximation. Technically, this is performed by looking for the value of α_4 such that a reduction of it by half results in a change of the stress–strain relation less than 5%.

The parameters ζ and μ can be considered as *material parameters*. They determine the constitutive response of the system, so they must be adjusted to the experimental data. In this study, we have adjusted them by comparing the simulation of biaxial tests of dense polygonal packings with the corresponding biaxial tests with dense Hostun sand [38]. First, the initial Young modulus of the material is linearly related to the value of normal stiffness of the contact. Thus, $k_n = 160$ MPa is chosen by fitting the initial slope of the stress–strain relation in the biaxial test. Then, the Poisson ratio depends on the ratio $\zeta = k_t/k_n$. Our choice $k_t = 52{\cdot}8$MPa gives an initial Poisson ratio of 0·2. This is obtained from the initial slope of the curve of volumetric strains versus axial strain. The angles of friction and the dilatancy are increasing functions of the friction coefficient μ. Taking $\mu = 0{\cdot}25$ yields angles of friction of 30–40 degrees and dilatancy angles of 10–20 degrees, which are similar to the experimental data of river sand [39].

4.4. Sample preparation

The Voronoi construction presented above leads to samples with no porosity. This ideal case contrasts with realistic soils, where only porosities up to a certain value can be achieved. In this section, we present a method to create stable, irregular packings of polygons with a given porosity.

The porosity can be defined using the concept of void ratio. This is defined as the ratio of the volume of the void space to the volume of the solid material. It can be calculated as:

$$\nu = \frac{V_t}{V_f - V_0} - 1. \tag{45}$$

This is given in terms of the area enclosed by the walls V_t, the sum of the areas of the polygons V_f and the sum of the overlapping areas between them V_0.

Of course, there is a maximal void ratio that can be achieved, because it is impossible to pack particles with an arbitrarily high porosity. The maximal void ratio ν_m can be detected by moving the walls until a certain void ratio is reached. We find a critical value, above which the particles can be arranged without touching. Since there are no contacts, the assembly cannot support a load, and even applying gravity will cause it to compactify. For a void ratio below this critical value, there will be particle overlap, and the assembly is able to sustain a certain load. This maximal value is around 0·28.

The void ratio can be decreased by reducing the volume between the walls. The drawback of this method is that it leads to significant differences between the inner and outer parts of the boundary assembly and hence unrealistic overlaps between the particles, giving rise to enormous pressures. Alternatively, one can confine the polygons by applying gravity to the particles and on the walls. Particularly, homogeneous, isotropic assemblies, as shown in Figure 6 can be generated by a gravitational field $\mathbf{g} = -g\mathbf{r}$, where $\mathbf{r}$ is the vector connecting the center of mass of the assembly to the center of the polygon.

When the sample is consolidated, repeated shear-stress cycles are applied from the walls, superimposed to a confining pressure. The external load is imposed by applying a force $[p_c + q_c \sin(2\pi t/t_0)]W$ and $[p_c + q_c \cos(2\pi t/t_0)]H$ on the horizontal and vertical walls, respectively. Here W and H are the width and the height of the sample, respectively. If we take $p_c = 16\,\text{kPa}$ and $q_c < 0{\cdot}4p_c$, we observe that the void ratio decreases as the number of cycles increases. Void ratios of around 0·15 can be obtained. It is worth mentioning that after some thousands of cycles the void ratio is still slowly decreasing, making it difficult to identify this minimal value.

5. Simulation results

In order to investigate different aspects of the incremental response, some numerical simulations were performed. Different polygonal assemblies of 400 particles were used in the calculations. The loading between two stress states was controlled by applying forces $[\sigma_1^i + (\sigma_1^f - \sigma_1^i)r(t)]W$ and $[\sigma_2^i + (\sigma_2^f - \sigma_2^i)r(t)]H$. A smooth modulation $r(t) = (1 - \cos(2\pi t/t_0))/2$ is chosen in order to minimize the acoustic waves produced during loading. The initial void ratio is around $\nu = 0{\cdot}22$.

The components of the stress are represented by $p = (\sigma_1 + \sigma_2)/2$ and $q = (\sigma_1 - \sigma_2)/2$, where σ_1 and σ_2 are the eigenvalues of the averaged stress tensor on the RVE. Equivalently, the coordinates of the strain are given by the sum $\gamma = \epsilon_2 - \epsilon_1$ and the difference $e = -\epsilon_1 - \epsilon_2$ of the eigenvalues of the strain tensor. We use the convention that $e > 0$ means compression of the sample. The diameter of the RVE is taken as $d = 16\ell$. All the calculations were taken in the quasistatic regime.

5.1. Superposition principle

We start by exploring the validity of the superposition principle presented in Subsection 3.3. Part (a) of Figure 7 shows the loading path during the proportional loading under constant

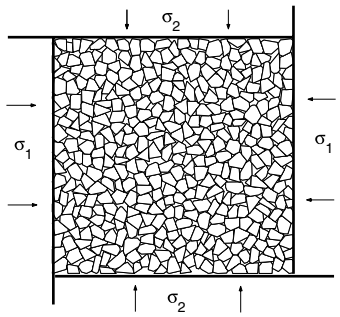

Figure 6. Polygonal assembly confined by a rectangular frame of walls.

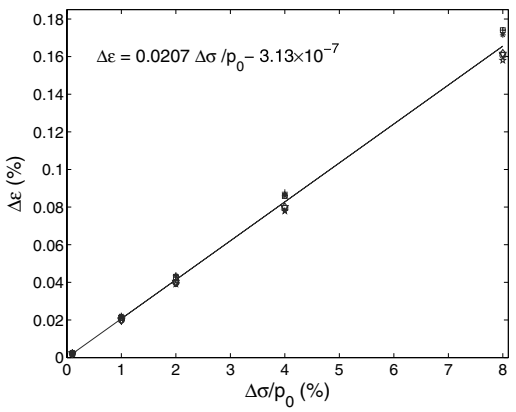

Figure 8. Distance between the response of the stair-like path and the proportional path.

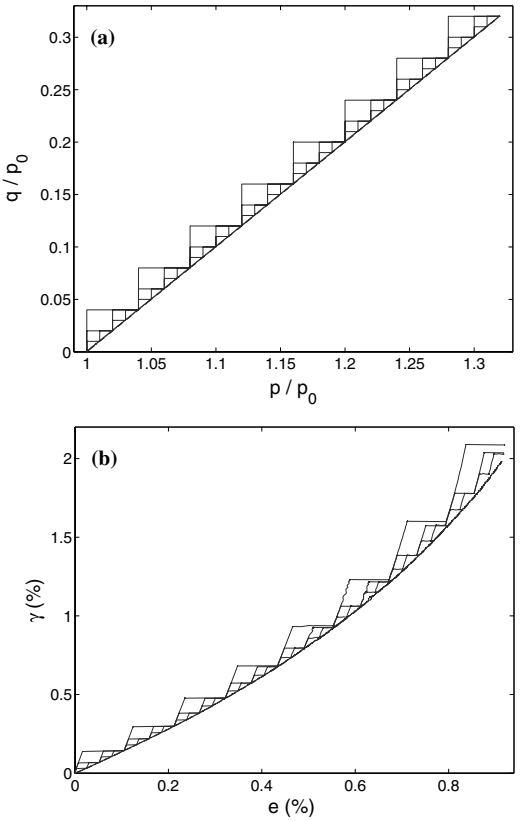

Figure 7. Numerical responses obtained from MD simulations of a rectilinear proportional loading (with constant lateral pressure) and stair-like paths. (a) Loading stress paths. (b) corresponding strain responses.

lateral pressure. This path is also decomposed into pieces divided into two parts: one is an incremental isotropic loading ($\Delta p = \Delta\sigma$ and $\Delta q = 0$), the other an incremental pure-shear loading ($\Delta q = \Delta\sigma$ and $\Delta p = 0$). The length of the steps $\Delta\sigma$ varies from to $0{\cdot}4p_0$ to $0{\cdot}001p_0$, where $p_0 = 640\,\text{kPa}$. Part (b) of Figure 7 shows that, as the steps decrease, the strain response converges to the response of the proportional loading. In order to verify this convergence, we calculate the difference between the strain response of the stair-like path $\gamma(e)$ and the proportional loading path $\gamma_0(e)$ as:

$$\Delta\epsilon \equiv \max_e |\gamma(e) - \gamma_0(e)|, \tag{46}$$

for different steps sizes. This is shown in Figure 8 for seven different polygonal assemblies. The linear interpolation of this data intersects the vertical axis at 3×10^{-7}. Since this value is below the error given by the quasi-static approximation, which is 3×10^{-4}, the results suggest that the responses converge to that of the proportional load. Therefore we find that, within our error bars, the superposition principle is valid.

Close inspection of the incremental response will show that the validity of the superposition principle is linked to the existence of tensorial zones in the incremental-stress space. Prior to this, a short introduction to the strain envelope responses will be given.

5.2. Incremental response

A graphical illustration of the constitutive models can be given by employing the so-called *response envelopes*. They were introduced by Gudehus [18] as a useful tool to visualize the properties of a given incremental constitutive equation. The strain-envelope response is defined as the image $\{d\tilde{\epsilon} = \mathcal{G}(d\tilde{\sigma}, \tilde{\sigma})\}$ in the strain space of the unit sphere in the stress space, which becomes a potato-like surface in the strain space.

In practice, the determination of the stress-envelope responses is difficult because it requires one to prepare many samples with identical material properties. Numerical simulations result as an alternative to the solution of this problem. They allow one to create clones of the same sample, and to perform different loading histories in each one of them.

In the case of a plane-strain test, where there is no deformation in one of the spatial directions, the strain-envelope response can be represented in a plane. According to (36), this response results in a rotated, translated ellipse in the hypoplastic theory, whereas it is given by a continuous curve consisting of two pieces of ellipses in the elastoplasticity theory, as a result of (35). It is then of obvious interest to compare these predictions with the stress-envelope response of the experimental tests.

Figure 9 shows the typical strain response resulting from different stress-controlled loadings in a dense packing of polygons. Each point is obtained from the strain response in a specific direction of the stress space, with the same stress amplitude of $10^{-4}p_0$. We take $q_0 = 0{\cdot}45p_0$ and $p_0 = 160\,\text{kPa}$ in this calculation. The best fit of these results in the envelopes response of the elastoplasticity (two pieces of ellipses). For comparison the hypoplasticity (one ellipse) is also shown in Figure 9.

From these results we conclude that the elastoplasticity theory is more accurate in describing the incremental response of our model. One can draw the same conclusion by taking different strain values with different initial stress values [40]. These results have shown that the incremental response can be accurately described using the elastoplastic relation of Equation (35). The validity of this equation is supported by the existence of a well-defined flow rule for each stress state [41].

5.3. Yield function

In Subsection 3.2, we showed that the yield surface is an essential element in the formulation of the Drucker-Prager theory. This surface encloses a hypothetical region in the stress space where only elastic deformations are possible [19]. The determination of such a yield surface is essential to determine the dependence of the strain response on the history of the deformation.

We attempt to detect the yield surface by using a standard procedure proposed in experiments with sand [24]. Figure 10 shows this procedure. Initially the sample is subjected to an isotropic pressure. Then the sample is loaded in the axial direction until it reaches the yield-stress state with pressure p and deviatoric stress q. Since plastic deformation is found at this stress value, the point (p, q) can be considered as a classical yield point. Then, the Drucker-Prager theory assumes the existence of a yield surface containing this point. In order to explore the yield surface, the sample is unloaded in the axial direction until it reaches the stress point with pressure $p - \Delta p$ and deviatoric stress $q - \Delta p$ inside the elastic regime. Then the yield surface is constructed by re-loading in different directions in the stress space. In each direction, the new yield point must be detected by a sharp change of the slope in the stress-strain curve, indicating plastic deformations.